Gear Tooth Profile Determination From Arbitrary Rack Geometry

Sandeep M. Vijayakar,
Biplab Sarkar,
Donald R. Houser,
The Ohio State University, Columbus, Ohio

Abstract:

This article describes a method of obtaining gear tooth profiles from the geometry of the rack (or hob) that is used to generate the gear. This method works for arbitrary rack geometries, including the case when only a numerical description of the rack is available. Examples of a simple rack, rack with protuberances and a hob with root chamfer are described. The application of this technique to the generation of boundary element meshes for gear tooth strength calculation and the generation of finite element models for the frictional contact analysis of gear pairs is also described.

Introduction

After selection of the basic gear tooth geometry, the proper design of the tooth profile is probably the next most important factor in successful gear design. Aspects of proper gear design, such as the minimization of the transmission error to reduce noise, load sharing between teeth, the strength of the teeth and the stresses in the fillet all depend upon the tooth profile and root geometry. Procedures that compute the transmission error need an accurate numercial description of the gear tooth profile, as do gear tooth strength calculating methods, such as boundary element and finite element methods, which need accurate load sharing information and rely heavily on the accuracy of the tooth profile itself. They also need accurate numercial descriptions of the gear tooth fillet. An approximate fillet description, such as a circular arc of an approximately

AUTHORS:

DR. SANDEEP M. VIJAYAKAR *received his BTech degree from the Indian Institute of Technology at Bombay and his M.S. and Ph.D. from Ohio State University. He is currently a research associate at Ohio State and a member of ASME.*

DR. DONALD R. HOUSER *is on the faculty of the Department of Mechanical Engineering, Ohio State University. In addition to his teaching responsibilities, he has researched and published in the areas of gear dynamics and noise, v-belts, vibration diagnostics and vibration signal analysis. He is also currently director of the university's Gear Dynamics and Gear Noise Research Laboratory. Dr. Houser is a member of ASME, SAE, AGMA and Tau Beta Pi, Pi Tau Sigma and Sigma Xi honorary fraternities. He is also chairman of the ASME Power Transmission and Gearing Committee. Dr. Houser received his degrees in Mechanical Engineering from the University of Wisconsin at Madison.*

BIPLAB SARKAR *received his Bachelor of Technology in mechanical engineering in 1985 from the Indian Institute of Technology, Kharagpur, India, and his Master of Science degree in 1988 from The Ohio State University. He is currently working on a doctorate in mechanical engineering at The Ohio State University. His areas of interest include gear manufacture and measurement and CAD/CAM.*

computed radius, is not adequate for this purpose.

When a gear is generated by a rack (which includes a hob) with straight sides and circular corners, the tooth profile is an involute with trochoids at the fillets. The equations for such a gear can be obtained in analytical form, such as in the text by Colbourne.[1] In practice, however, various modifications, such as protuberances and profile modifications, may be applied to the rack. The corner of the hob itself need not be circular, and there may be a chamfer of specified dimensions. In such cases, it is not always possible to come up with an analytical form for the gear tooth profile.

Chang et al.[2] described a methodology to generate the involute profile on a computer from a straight sided rack. Hefeng et al.[3] described a technique that would also generate the trochoidal portion of the gear tooth profile which is generated by the circular corners at the tip of the rack. In the technique described in that article, for every relative orientation of the gear with respect to the rack, a point on the gear was found at which the normal passed through the pitch point, thus generating the profile. This technique, however, required an analytical description of the rack tooth profile. When the rack tooth profile is defined numerically or when the rack profile is more complicated than a set of straight lines and circles, the method was found to be difficult to use.

In this article, a method is described which is general enough to numerically compute the gear tooth profile of a generated gear tooth, given the geometry of the rack. Instead of searching along the rack profile to find a point which satisfies the meshing condition for a fixed relative orientation, this method determines the relative orientation of the gear and the rack for which a fixed point on the rack satisfies the condition of meshing. This method is more amenable to dealing with complicated rack profiles for which closed form equations are either not available or are too cumbersome to work with. It can also take into account the undercutting in gears. Even though it is not presented here, the method is also applicable to shaper cut geometries.

Profile Generation Algorithm

The input data required for this algorithm consist of a description of the rack that generates the gear, the number of teeth on the gear and the outer diameter of the gear. Fig. 1 shows a coordinate system $\underline{X}_r$ attached to a rack. The origin of this coordinate system lies on the pitch line of the rack. Let $\underline{x}_r = (x_r, y_r)$ be the coordinates of an arbitrary point P on the rack profile, with respect to the coordinate system $\underline{X}_r$ attached to the rack. Let $\underline{n}_r = (n_x, n_y)$ be the outward unit normal to the rack at this point. For any specified rack geometry, the coordinates and the normal vector at any point on the rack profile are easily obtained.

Fig. 2 shows a gear tooth with an attached coordinate system $\underline{X}_g$ with its origin at the center of the gear. Let P′ be a point on the gear tooth profile that corresponds to the point P on the rack. In other words, as the gear rolls through with the rack, the point P on the rack makes sliding contact with the point P′ on the gear. Let $\underline{x}_g = (x_g, y_g)$ be the coordinates of the point P′ on the gear with respect to the coordinate system $\underline{X}_g$ attached to the gear.

This algorithm uses the coordinate and unit normal vector data available for the point P to compute the coordinates of the point P′. Fig. 3 shows the relative position of the gear and rack

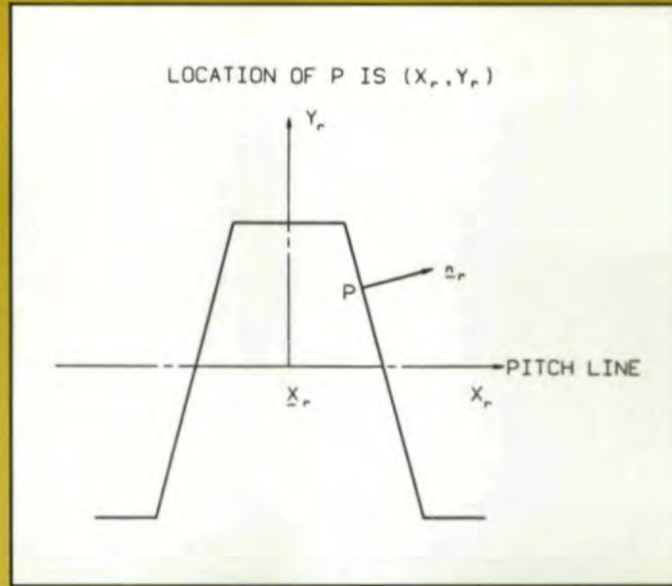

Fig. 1 – The rack and its attached coordinate system.

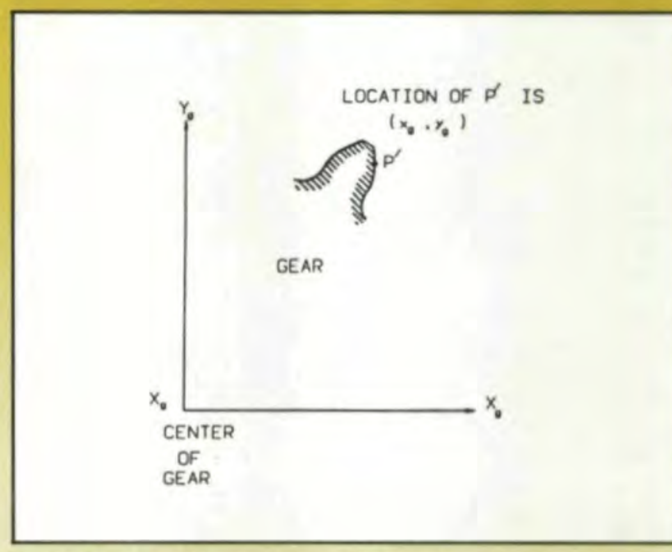

Fig. 2 – The gear and its attached coordinate system.

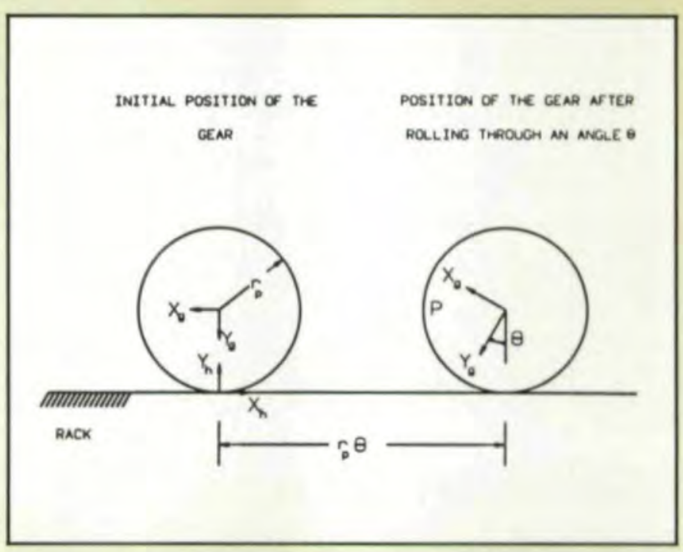

Fig. 3 – The relative orientation of the gear and rack coordinates systems during generation.

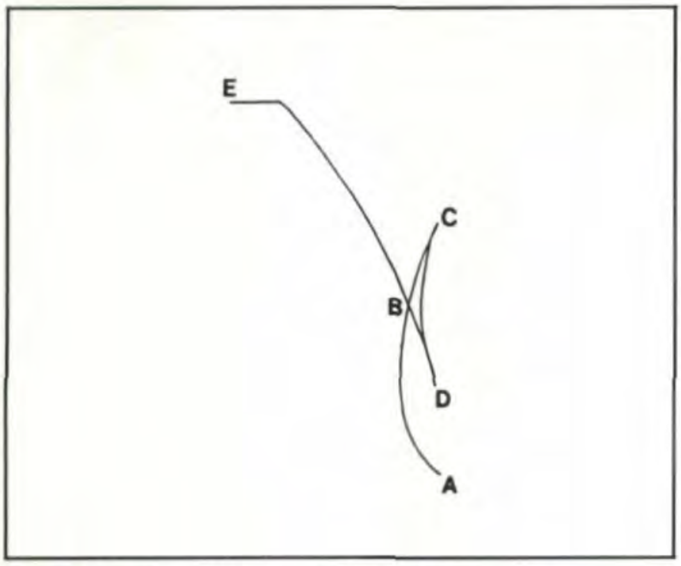

Fig. 4 – Gear tooth profile generated when undercutting occurs.

at a starting position and at a position after the gear has rolled through an angle θ. The pitch circle radius of the gear is r. For this arbitrary orientation of the gear, the transformation from the rack coordinate system to the gear coordinate system is defined by the matrix equation:

$$\begin{Bmatrix} x_g \\ y_g \end{Bmatrix} = \begin{bmatrix} -\cos\theta & \sin\theta \\ -\sin\theta & -\cos\theta \end{bmatrix} \begin{Bmatrix} x_r - r\theta \\ y_r - r \end{Bmatrix} \qquad (1)$$

As the gear rolls, the relative velocity of the point P′ on the gear with respect to the rack is

$$\underline{v} = \begin{Bmatrix} r\dot{\theta} \\ 0 \end{Bmatrix} + \dot{\theta} \begin{Bmatrix} y_r - r \\ r\theta - x_r \end{Bmatrix}$$

the first part being the translational contribution, and the second part being the rotational contribution. $\dot{\theta}$ is the time derivative of θ. Hence,

$$\underline{v} = \dot{\theta} \begin{Bmatrix} y_r \\ r\theta - x_r \end{Bmatrix}$$

According to the equation of meshing, this relative velocity of the point on the gear should have no component normal to the rack, such that the dot product

$$\underline{v} \cdot \begin{Bmatrix} n_x \\ n_y \end{Bmatrix} = 0$$

or,

$$y_r n_x + (r\theta - x_r)\, n_y = 0$$

Thus the roll angle at which the point P makes contact with a point on the gear is given by

$$\theta = \frac{x_r n_y - y_r n_x}{r n_y} \qquad (2)$$

Given any point P on the rack, its coordinates and its normal vector, the roll angle at which it makes contact with the gear can be computed from Equation 2. The coordinates of the corresponding point P on the gear can then be obtained by substituting for θ in Equation 1. Therefore, a sequence of points on the gear tooth profile can be found that correspond to a sequence of points on the rack profile.

The next step is to examine the gear tooth profile thus obtained for possible undercutting. If undercutting does take place, the gear tooth profile will look like Fig. 4. The part B-C-D-B has to be detected, and the points in this part have to be eliminated from the sequence of points that define the profile of the gear tooth.

Let $\{\underline{r}_i, i=1,n\}$ be a sequence of coordinates corresponding to the points on the gear tooth profile. To detect the cross-over point B shown in Fig. 4, we need to check whether there exist integers i and j such that the line segment $(i, i+1)$, which joins $\underline{r}_i$ with point $\underline{r}_{i+1}$ intersects the line segment $(j-1, j)$. Fig. 5 shows two line segments, (a,b) and (c,d). These line segments will in-

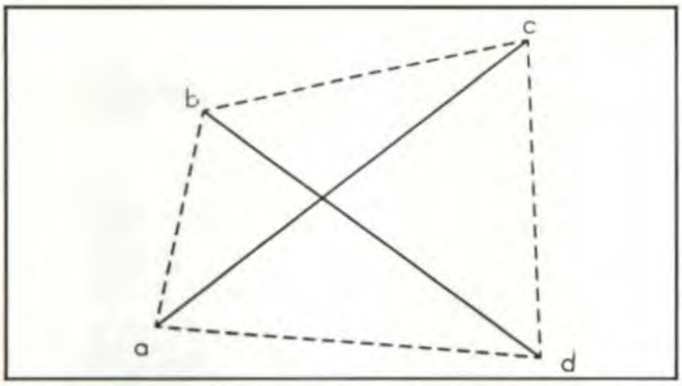

Fig. 5 – Determination of the point of intersection of two line segments.

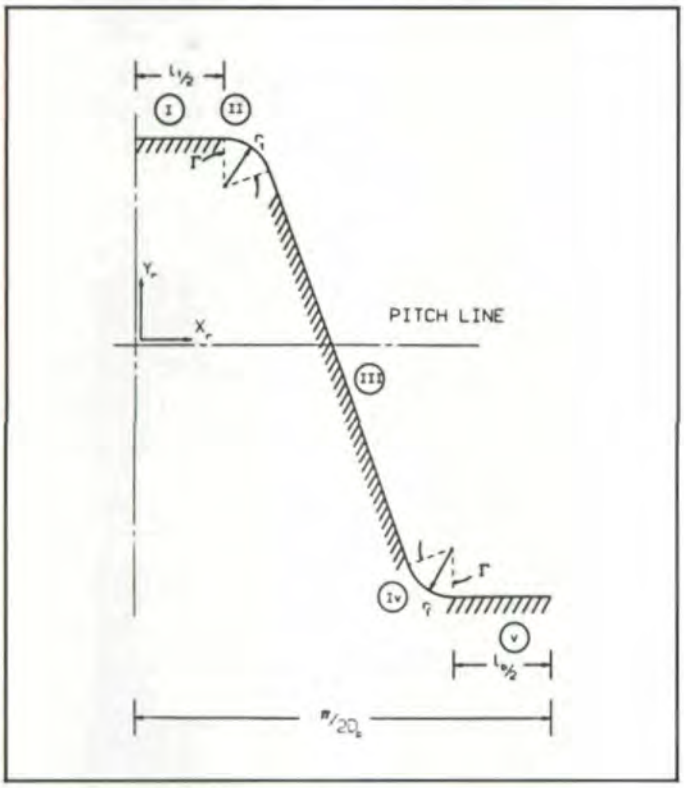

Fig. 6 – Geometry of an elementary rack.

tersect if and only if

$$A(a,b,c) \cdot A(a,b,d) < 0$$

and

$$A(c,d,a) \cdot A(c,d,b) < 0$$

where

$$A(a,b,c) = (\underline{r}_b - \underline{r}_a) \times (\underline{r}_c - \underline{r}_a)$$

where $\underline{r}_a$, $\underline{r}_b$, and $\underline{r}_c$ are three-dimensional coordinates of the three points a, b and c, respectively; the "x" stands for a vector cross product and the · stands for the vector inner product.

$$\underline{r}_a = \begin{Bmatrix} x_a \\ y_a \\ 0 \end{Bmatrix}, \underline{r}_b = \begin{Bmatrix} x_b \\ y_b \\ 0 \end{Bmatrix} \text{ and}$$

$$\underline{r}_c = \begin{Bmatrix} x_c \\ y_c \\ 0 \end{Bmatrix}$$

The location of the point of intersection $\underline{r}_e$ will be

$$\underline{r}_e = \alpha\,\underline{r}_a + (1 - \alpha)\underline{r}_b$$

where $$\alpha = \frac{\| A(c,d,b,) \|}{\| A(c,d,a) \| + \| A(c,d,b) \|}$$

Using this method, the whole profile can be searched for segments (i,i+1) and (j−1,j) that intersect. If such an i and j are found, then all points on the profile between i+1 and j−1 are discarded and replaced by a single point, the point of intersection.

A similar condition occurs at the tip of the gear tooth when the radius at the root of the rack profile is not large enough, or when there is a chamfer at the root of the rack profile. The same technique can be used to eliminate points that cannot possibly lie on the gear tooth.

Geometry of a Simple Rack. Fig. 6 shows a simple rack.

Let D_p = Diametral pitch,
A = Addendum,
B = Dedendum,
ϕ = Pressure angle,
r_t = Radius at tip of rack tooth,
r_f = Radius at fillet of rack tooth,

$$\Gamma = \frac{\pi}{2} - \phi$$

$$l_t = \frac{\pi}{2D_p} - 2A\tan(\phi) - 2r_t\tan\left(\frac{\Gamma}{2}\right)$$

$$l_b = \frac{\pi}{2D_p} - 2B\tan(\phi) - 2r_f\tan\left(\frac{\Gamma}{2}\right)$$

Coordinates of points along the rack profile are then given by:

In region I (the top land),

$$\begin{Bmatrix} x_r \\ y_r \end{Bmatrix} = \begin{Bmatrix} \beta l_t/2 \\ A \end{Bmatrix}$$

$$\begin{Bmatrix} n_x \\ n_y \end{Bmatrix} = \begin{Bmatrix} 0 \\ 1 \end{Bmatrix} \quad 0 < \beta \leq 1$$

In region II (the tip radius),

$$\begin{Bmatrix} x_r \\ y_r \end{Bmatrix} = \begin{Bmatrix} l_t/2 + r_t\sin(\beta\Gamma] \\ A - r_t(1 - \cos(\beta\Gamma)) \end{Bmatrix}$$

$$\begin{Bmatrix} n_x \\ n_y \end{Bmatrix} = \begin{Bmatrix} \mathrm{Sin}(\beta\Gamma) \\ \mathrm{Cos}\,(\beta\Gamma) \end{Bmatrix} \quad 0 < \beta \leq 1$$

In region III (the tooth flank),

$$\begin{Bmatrix} x_r \\ y_r \end{Bmatrix} = (1-\beta) \begin{Bmatrix} l_t/2 + r_t\sin\Gamma \\ A - r_t(1 - \cos\Gamma) \end{Bmatrix}$$

$$+ \beta \begin{Bmatrix} \pi/2D_p - l_b/2 - r_f\mathrm{Sin}\Gamma \\ -B + r_f(1\text{-}\cos\Gamma) \end{Bmatrix}$$

$$\begin{Bmatrix} n_x \\ n_y \end{Bmatrix} = \begin{Bmatrix} \text{Cos}\phi \\ \text{Sin}\phi \end{Bmatrix} \; 0<\beta\leq 1$$

In region IV (the root fillet),

$$\begin{Bmatrix} x_r \\ y_r \end{Bmatrix} = \begin{Bmatrix} \pi/2D_p - l_b/2 - r_f\text{Sin}((1-\beta)\Gamma) \\ -B + r_f(1-\cos((1-\beta)\Gamma) \end{Bmatrix}$$

$$\begin{Bmatrix} n_x \\ n_y \end{Bmatrix} = \begin{Bmatrix} \text{Sin}((1-\beta)\Gamma) \\ \text{Cos}((1-\beta)\Gamma) \end{Bmatrix} \; 0<\beta\leq 1$$

In region V (the bottom land),

$$\begin{Bmatrix} x_r \\ y_r \end{Bmatrix} = \begin{Bmatrix} \pi/2D_p - (l_b/2)(1-\beta) \\ -B \end{Bmatrix}$$

$$\begin{Bmatrix} n_x \\ n_y \end{Bmatrix} = \begin{Bmatrix} 0 \\ 1 \end{Bmatrix} \; 0<\beta\leq 1$$

<u>Geometry of a Rack with Protuberance.</u> Fig. 7 shows a rack with protuberance.

Let α = Protuberance angle,

d = Protuberance high point distance,

l = Parallel land length,

$$l_t = \frac{\pi}{2D_p} - 2A\tan(\phi) - 2r_t\tan(\frac{\Gamma}{2}) + 2(\frac{d}{\cos\phi})$$

$$l_b = \frac{\pi}{2\,D_p} - 2B\tan(\phi) - 2r_f\tan(\frac{\Gamma}{2})$$

Coordinates of points along the profile of the rack with protuberance are then given by:

In region I (the top land),

$$\begin{Bmatrix} x_r \\ y_r \end{Bmatrix} = \begin{Bmatrix} \beta l_t/2 \\ A \end{Bmatrix}$$

$$\begin{Bmatrix} n_x \\ n_y \end{Bmatrix} = \begin{Bmatrix} 0 \\ 1 \end{Bmatrix} \; 0<\beta\leq 1$$

In region II (the tip radius),

$$\begin{Bmatrix} x_r \\ y_r \end{Bmatrix} = \begin{Bmatrix} l_t/2 + r_t\sin(\beta\Gamma) \\ A - r_t(1-\cos(\beta\Gamma)) \end{Bmatrix}$$

$$\begin{Bmatrix} n_x \\ n_y \end{Bmatrix} = \begin{Bmatrix} \text{Sin}(\beta\Gamma) \\ \text{Cos}(\beta\Gamma) \end{Bmatrix} \; 0<\beta\leq 1$$

In region III (the parallel land),

$$\begin{Bmatrix} x_r \\ y_r \end{Bmatrix} = \begin{Bmatrix} l_t/2 + r_t\sin\Gamma + \beta l\sin\phi \\ A - r_t(1-\cos\Gamma) - \beta l\cos\phi \end{Bmatrix}$$

$$\begin{Bmatrix} n_x \\ n_y \end{Bmatrix} = \begin{Bmatrix} \cos\phi \\ \sin\phi \end{Bmatrix} \; 0<\beta\leq 1$$

In region IV (protuberance angle length),

$$\begin{Bmatrix} x_r \\ y_r \end{Bmatrix} = \begin{Bmatrix} l_t/2 + r_t\sin\Gamma + l\sin\phi \\ A - r_t(1-\cos\Gamma) - l\cos\phi \end{Bmatrix} + \beta \begin{Bmatrix} (d/\sin\alpha)\sin(\phi-\alpha) \\ -(d/\sin\alpha)\cos(\phi-\alpha) \end{Bmatrix}$$

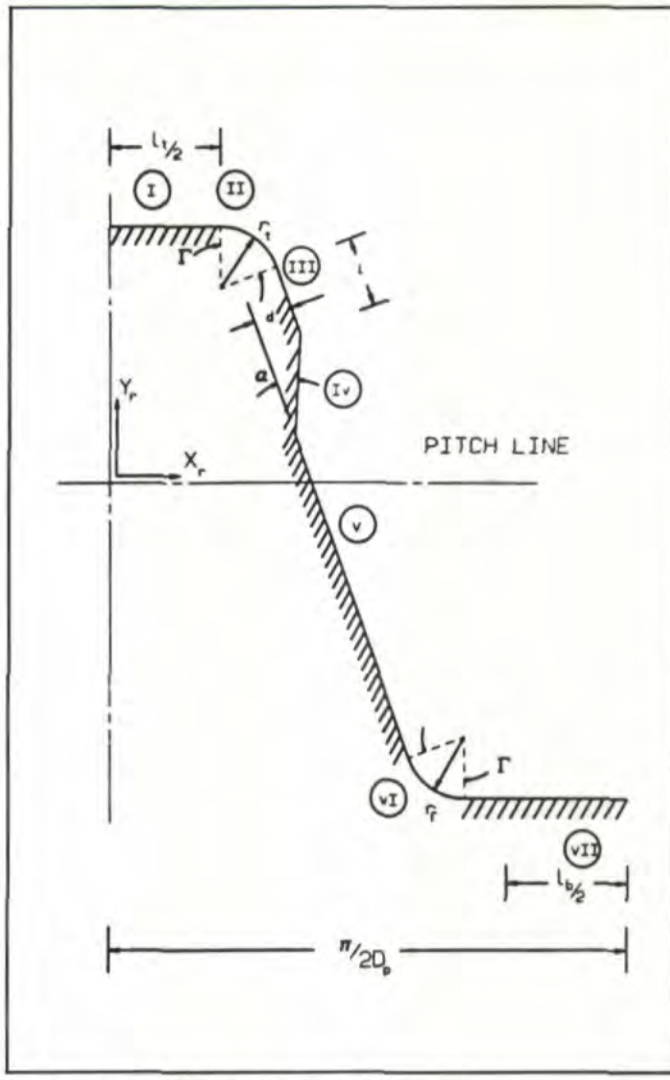

Fig. 7 – Geometry of a rack with a protuberance.

$$\begin{Bmatrix} n_x \\ n_y \end{Bmatrix} = \begin{Bmatrix} \cos(\phi-\alpha) \\ \sin(\phi-\alpha) \end{Bmatrix} \; 0<\beta\leq 1$$

In region V (the tooth flank),

$$\begin{Bmatrix} x_r \\ y_r \end{Bmatrix} = (1-\beta)\begin{Bmatrix} l_t/2 + r_t\sin\Gamma + l\sin\phi \\ A - r_t(1-\cos\Gamma) - l\cos\phi \end{Bmatrix} + (1-\beta)(d/\sin\alpha)\begin{Bmatrix} \sin(\phi-\alpha) \\ -\cos(\phi-\alpha) \end{Bmatrix} + \beta\begin{Bmatrix} \pi/2D_p - l_b/2 - r_f\text{Sin}\Gamma \\ -B + r_f(1-\cos\Gamma) \end{Bmatrix}$$

$$\begin{Bmatrix} n_x \\ n_y \end{Bmatrix} = \begin{Bmatrix} \cos\phi \\ \sin\phi \end{Bmatrix} \; 0<\beta\leq 1$$

In region VI (the root fillet),

$$\begin{Bmatrix} x_r \\ y_r \end{Bmatrix} =$$

$$\begin{Bmatrix} \pi/2D_p - l_b/2 - r_f\mathrm{Sin}((1-\beta)\Gamma) \\ -B + r_f(1-\cos((1-\beta)\Gamma) \end{Bmatrix}$$

$$\begin{Bmatrix} n_x \\ n_y \end{Bmatrix} = \begin{Bmatrix} \mathrm{Sin}((1-\beta)\Gamma) \\ \mathrm{Cos}((1-\beta)\Gamma) \end{Bmatrix} \quad 0<\beta\leq 1$$

In region VII (the bottom land),

$$\begin{Bmatrix} x_r \\ y_r \end{Bmatrix} = \begin{Bmatrix} \pi/2D_p - (l_b/2)(1-\beta) \\ -B \end{Bmatrix}$$

$$\begin{Bmatrix} n_x \\ n_y \end{Bmatrix} = \begin{Bmatrix} 0 \\ 1 \end{Bmatrix} \quad 0<\beta\leq 1$$

Geometry of a Hob with Root Chamfer. Often hobs with root chamfers are used to provide tip relief on the gear. Fig. 8 shows such a hob with a chamfer. Then

$$l_t = \frac{\pi}{2D_p} - 2A\tan(\phi) - 2r_t\tan(\frac{\Gamma}{2})$$

$$l_b = \frac{\pi}{2D_p} - 2B\tan(\phi)$$

$$- 2L_1(\tan\eta - \tan\phi)$$

where $\eta = \tan^{-1}(L_2/L_1)$

where L_1 and L_2 define the root chamfer as shown in Fig. 8. Coordinates of points along the rack profile are then given by:

In region I (the top land),

$$\begin{Bmatrix} x_r \\ y_r \end{Bmatrix} = \begin{Bmatrix} \beta l_t/2 \\ A \end{Bmatrix}$$

$$\begin{Bmatrix} n_y \\ n_y \end{Bmatrix} = \begin{Bmatrix} 0 \\ 1 \end{Bmatrix} = 0<\beta\leq 1$$

In region II (the tip radius),

$$\begin{Bmatrix} x_r \\ y_r \end{Bmatrix} = \begin{Bmatrix} l_t/2 + r_t\sin(\beta\Gamma) \\ A - r_t(1-\cos(\beta\Gamma)) \end{Bmatrix}$$

$$\begin{Bmatrix} n_x \\ n_y \end{Bmatrix} = \begin{Bmatrix} \mathrm{Sin}\,(\beta\Gamma) \\ \mathrm{Cos}\,(\beta\Gamma) \end{Bmatrix} \quad 0<\beta\leq 1$$

In region III (the tooth flank),

$$\begin{Bmatrix} x_r \\ y_r \end{Bmatrix} = (1-\beta)\begin{Bmatrix} l_t/2 + r_t\sin\Gamma \\ A - r_t(1-\cos\Gamma) \end{Bmatrix}$$

$$+ \beta\begin{Bmatrix} \pi/2D_p - l_b/2 - L_2 \\ -B + L_1 \end{Bmatrix}$$

$$\begin{Bmatrix} n_x \\ n_y \end{Bmatrix} = \begin{Bmatrix} \mathrm{Cos}\phi \\ \mathrm{Sin}\phi \end{Bmatrix} \quad 0<\beta\leq 1$$

In region IV (the root chamfer),

$$\begin{Bmatrix} x_r \\ y_r \end{Bmatrix} \begin{Bmatrix} \pi/2D_p - l_b/2 - L_2(1-\beta) \\ -B + L_1(1-\beta) \end{Bmatrix}$$

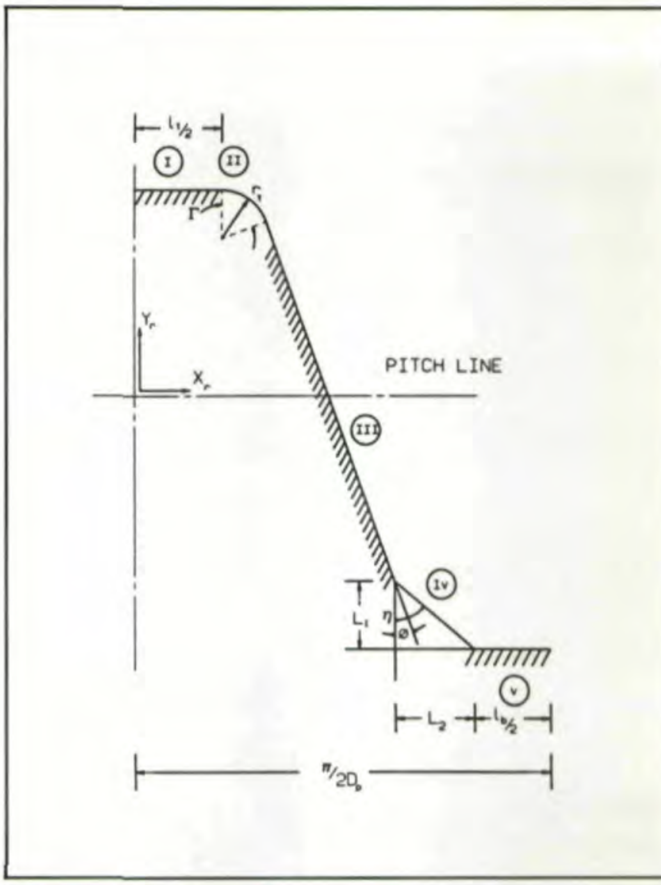

Fig. 8 – Geometry of a hob with root chamfer.

Vertical Hob Sharpener

For straight gash hobs up to 6-in. dia. by 6-in. long. Indexing accuracy for "Class A" tolerances without using index plates.

Star

SHARPENING

...the economical and
for your tool sharpen

Six-Axis CNC Tool Grinder

This six axis machine allows users to automatically resharpen tools to their original manufacturing specifications.

These domestically manufactured machines have fully programmable automatic grinding cycles and user needs are fully accommodated in their design. We provide on-site engineering service and training to our customers.

CNC Hob Sharpener

For straight gash hobs up to 10-in. dia. by 12-in. long. Indexing accuracy for "Class AA" tolerances without using change gears or index plates.

MACHINES

ractical solution
g requirements.

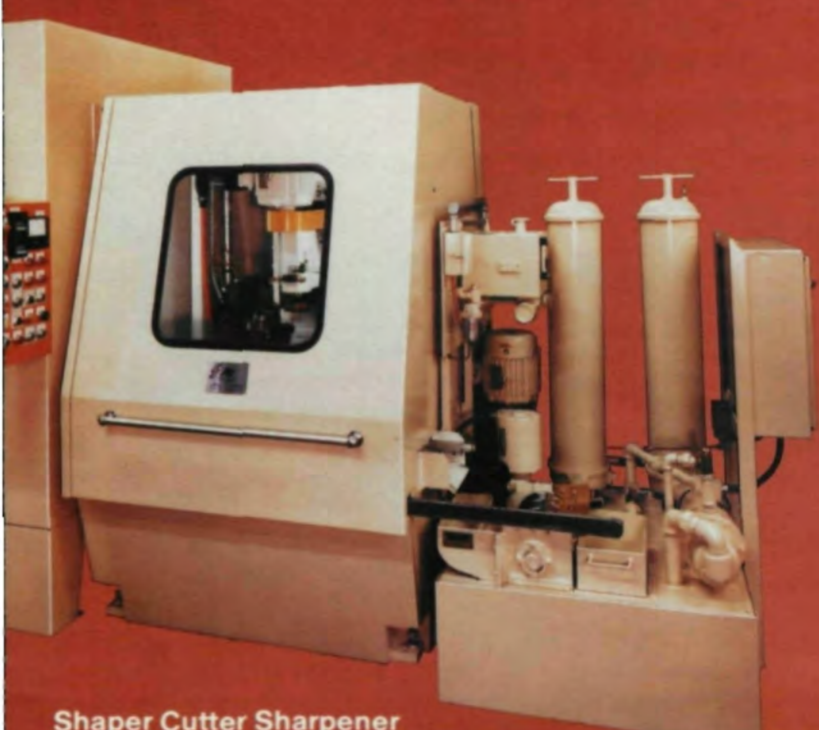

Shaper Cutter Sharpener

For both spur type and right- or left-hand helical type shaper cutters. Fully programmable, totally automatic cycles.

STARCUT SUPPLIED PRODUCTS AND SERVICES

Star Machine Tools
Standard and CNC Hob Sharpeners
Shaper Cutter Sharpeners
CNC Tool and Cutter Grinders (5-Axis and 6-Axis)

Star Cutting Tools
Hobs
Form-Relieved Cutters
Gun Drills
Gun Reamers
Keyseat Cutters

Gold Star Coatings

Hurth Machine Tools
CNC Gear Shaving Machines
CNC Gear Rolling Machines
Gear Testing Machines
Shaving Cutter Grinding Machines
CNC Gear Tooth Chamfering Machines
Gear Deburring Machines
CNC Hard Gear Finishing Machines

Mikron
Hobbing Machines
Hob Sharpener
Hobs
Shaper Cutters

TiN Coating Systems
Complete Turnkey Applications

Stieber
Precision Clamping Tools

Please contact us for further information on any or all of these sharpening machines and other StarCut supplied products and services.

Since 1927
Star

STARCUT SALES, INC.
23461 Industrial Park Drive
Farmington Hills, MI 48024
313/474-8200 Telex 230-411

CIRCLE A-18 ON READER REPLY CARD

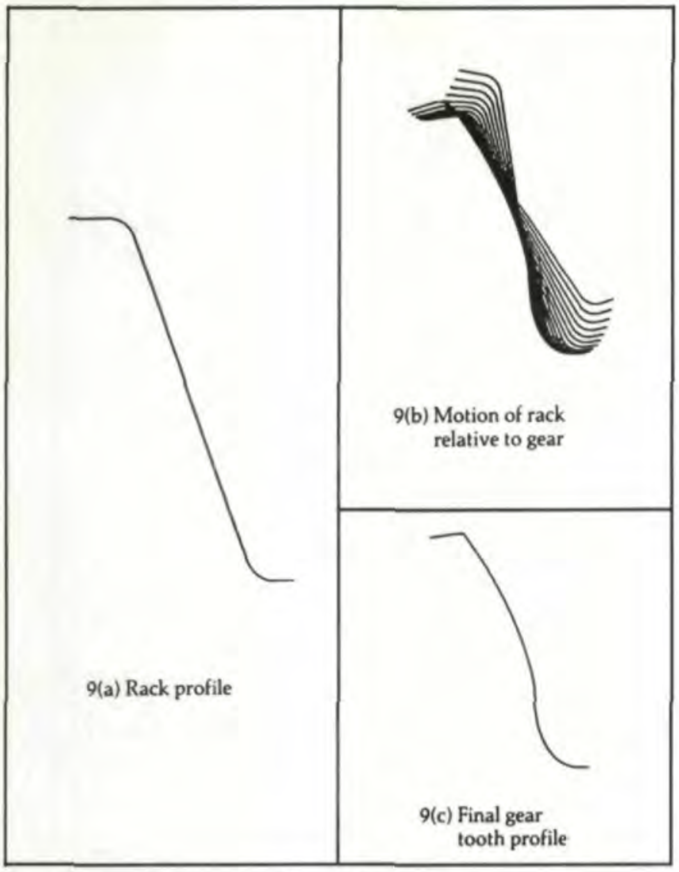

Fig. 9 – Generation of a gear with a simple rack.

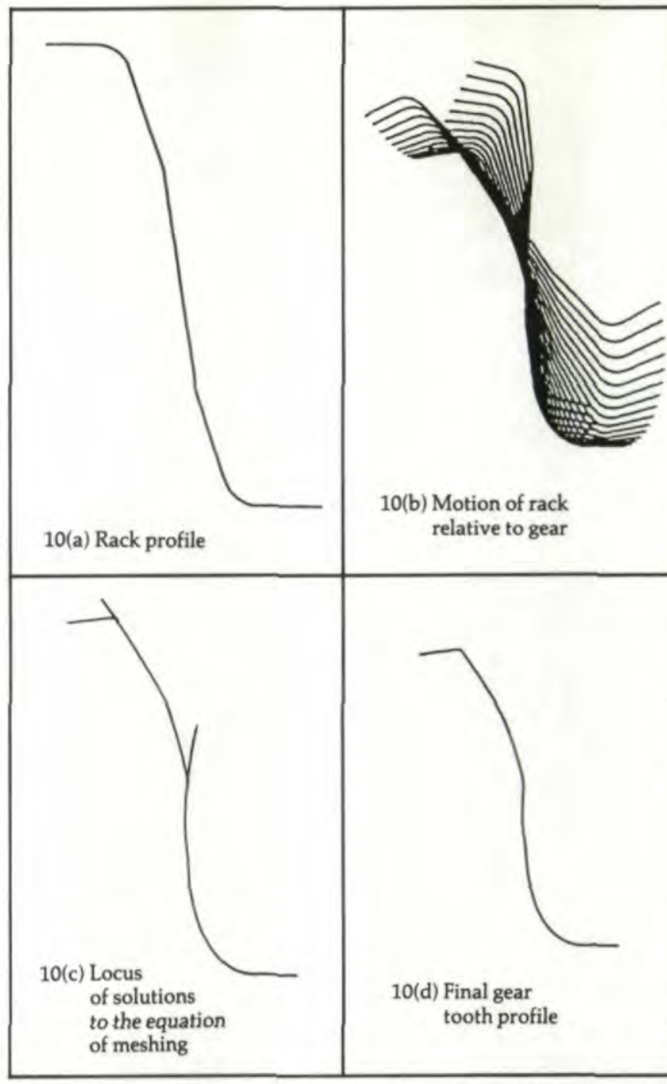

Fig. 10 – Generation of a gear using a rack with a protuberance angle $\alpha = 10°$.

$$\begin{Bmatrix} n_x \\ n_y \end{Bmatrix} = \begin{Bmatrix} \mathrm{Cos}\eta \\ \mathrm{Sin}\eta \end{Bmatrix} 0 < \beta \leq 1$$

In region V (the bottom land),

$$\begin{Bmatrix} x_r \\ y_r \end{Bmatrix} = \begin{Bmatrix} \pi/2D_p - (l_b/2)(1-\beta) \\ -B \end{Bmatrix}$$

$$\begin{Bmatrix} n_x \\ n_y \end{Bmatrix} = \begin{Bmatrix} 0 \\ 1 \end{Bmatrix} 0 < \beta \leq 1$$

Profile Generation Examples. Consider a basic rack with pressure angle $\phi = 20°$, with a diametral pitch $D_p = 10$ per inch, an addendum constant of 1.4, dedendum constant of 1.0 and a tip radius $r_t = 0.02''$.

Fig. 9(a) shows such a rack with no protuberance and with a root fillet radius $r_f = 0.02$ inches. Fig. 9(b) shows the positions of the rack relative to the generated gear as a gear with 20 teeth rolls through. Fig. 9(c) shows the gear tooth profile, which is obtained by using the procedure described earlier.

Fig. 10(a) shows the same rack, but with a protuberance angle $\alpha = 10°$, a parallel land length $l = 0.05$ inches and protuberance high point distance $d = 0.02$ inches. Fig. 10(b) shows the motion of the rack relative to the gear and Fig. 10(c) shows

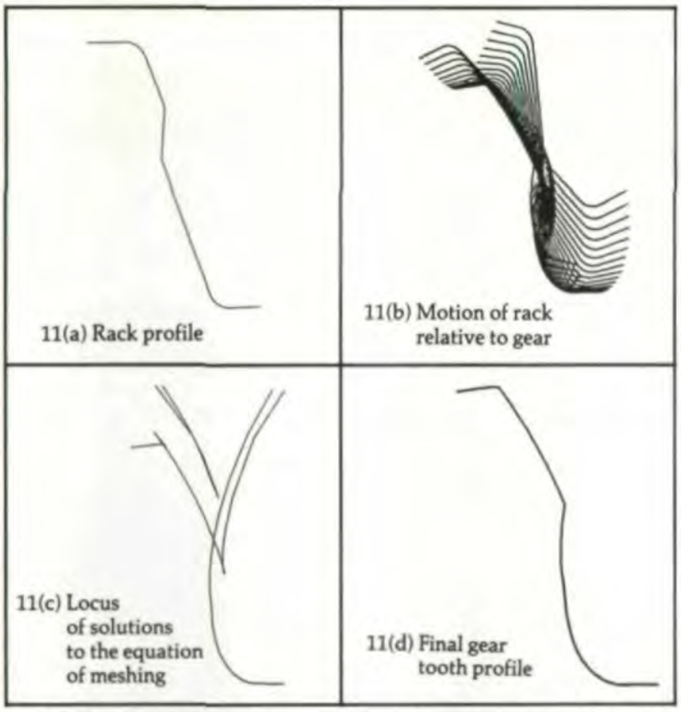

Fig. 11 – Generation of a gear using a rack with a protuberance angle $\alpha = 25°$.

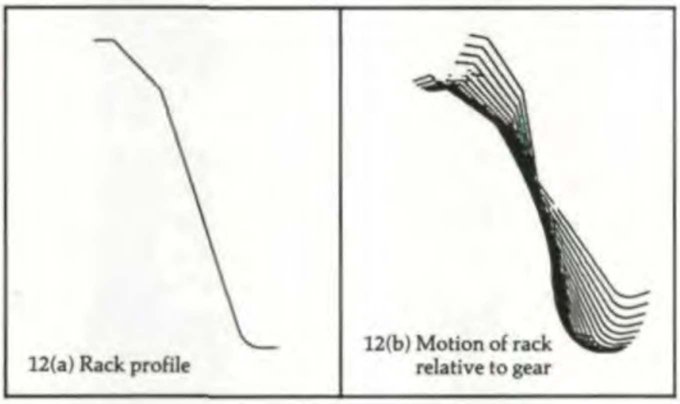

the locus of the points that are solutions to the equation of meshing. Note the severe undercutting and the presence of non-feasible points at the gear tooth tip and at the intersection of the involute section of the gear tooth profile with the trochoidal root. Fig. 10(d) shows the final profile, obtained after all non-feasible points have been eliminated using the procedure described earlier in this paper. Figs. 11(a) through (d) show the same process for an extremely exaggerated case with protuberance angle $\alpha = 25°$.

Figs. 12(a) through (d) show a similar hob with a root chamfer with intercepts $L_1 = 0.04''$ and $L_2 = 0.04''$. (See Fig. 8.)

In order to keep to the more practical rack geometries, the examples described here had rack profiles which were made up of straight lines and circles, but the method may be applied to arbitrary geometries with equal ease.

Applications.

a) In Computer-Aided Design Programs: The simplest use to which this procedure can be put is that of drawing gears for different rack geometries as part of general computer-aided design programs. It can show the severity of undercutting and allow the designer through the use of zoom features to accurately predict the shape of the tooth which is being developed. Fig. 13

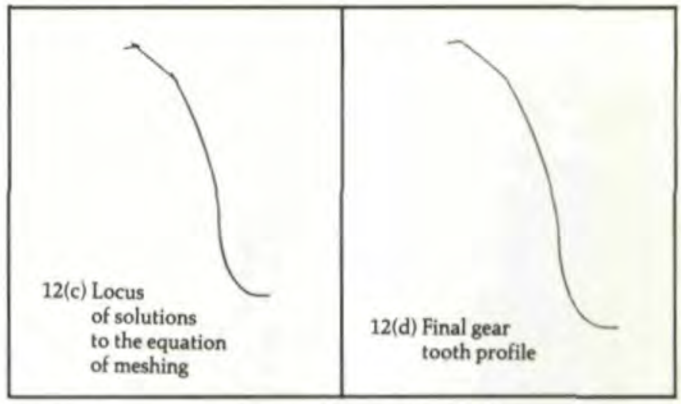

Fig. 12 – Generation of a gear using a rack with a chamfer.

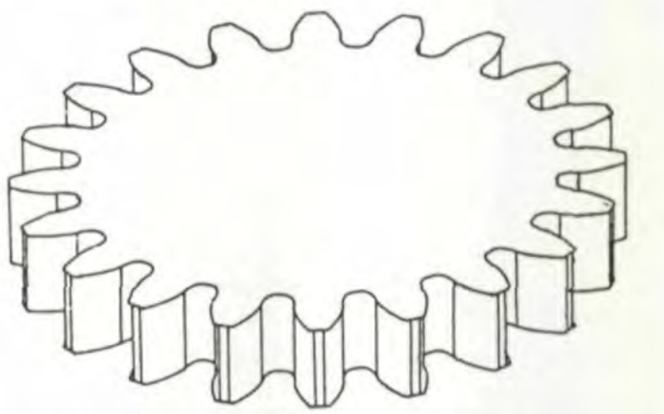

Fig. 13 – Perspective view of a gear with an automatically generated profile.

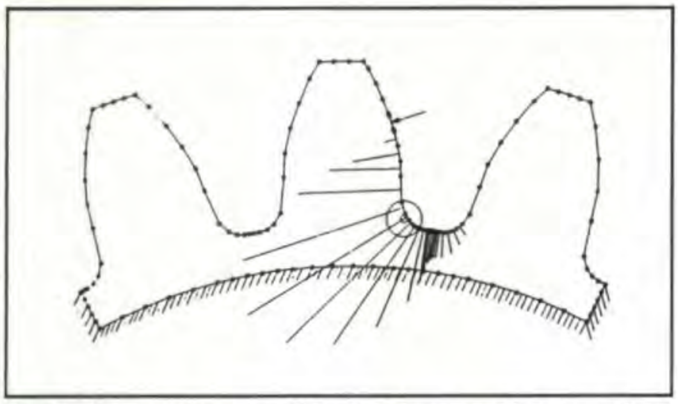

Fig. 14 – Automatically generated boundary element model of a non-undercut gear.

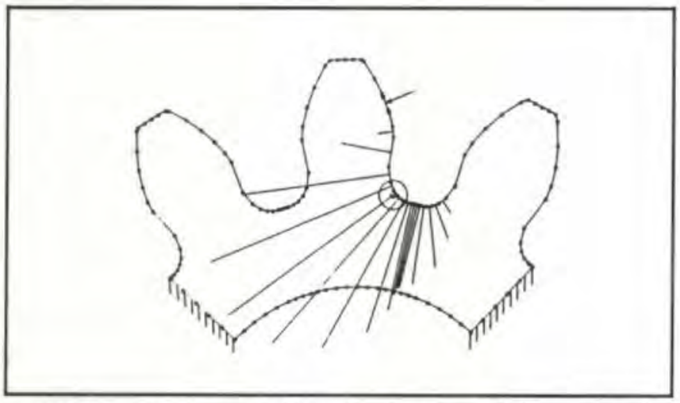

Fig. 15 – Automatically generated boundary element model of a severely undercut gear.

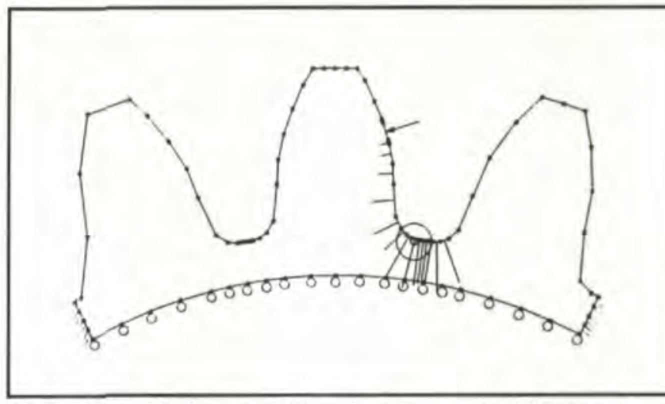

Fig. 16 – Automatically generated boundary element model of a non-undercut gear supported on rollers.

shows in perspective view a full gear with face width 0.3", which is being generated by the simple hob described before.

b) Generation of Boundary Element Meshes for Strength Computations: The estimation of the strength of a gear can be carried out in many different ways, of which the boundary element method is probably the most efficient and convenient. Because the boundary element method is very accurate, the stress concentration at the fillet of the gear tooth root is very sensitive to the correctness of the geometry of the fillet at the root of the gear tooth. The automatic gear profile generation procedure described in this article is very useful in generating boundary element models which accurately model the root geometries.

As described in an earlier article by Vijayakar and Houser, [4] the boundary element procedure can easily display stress variation along the boundary of the gear model, determine the location at which critical stresses occur and determine the AGMA geometry factor. The procedure also allows the computation of the state of stress at any prescribed point within the gear.

Several boundary conditions can be applied in the boundary element model of the gear teeth. The inner boundary and the sides can be fixed, or the inner boundary can be free, while the sides can be fixed, or else the inner boundary can be supported on rollers with the sides fixed. Figs. 14, 15 and 16 show the stress distribution along the boundaries of three thin-rimmed gears with different boundary conditions. The gear shown in Fig. 14 has no undercutting, and its inner rim and the sides are fixed, while the gear in Fig. 15 is severely undercut and has rigid side supports. Fig. 16 shows the stress distribution of another thin-rimmed gear with roller supported inner boundary and fixed sides.

c) Contact Analysis of Gears: Developments in the area of contact analysis of finite element models with friction have made it possible to determine the load dependent transmission error of gears in mesh by meshing finite element models of a pair of gears and turning them against each other in a simulation. However, the magnitude of the transmission error itself is typically very small.

Therefore, in order to carry out meaningful simulations of gears in mesh, where the error in the transmission error due to the finite element discretization of the gear profile is much smaller than the actual transmission error, it is imperative that the finite element model be able to model the geometry of the gear with a high degree of accuracy. In such a case, manual methods of model creation, such as using drawings and a digitizing tablet, are out of the question, and an automatic procedure such as that described in this article becomes essential.

As an example, consider a gear with 20 teeth, a diametral pitch of 10 per inch and a face width of one inch. Under a load of 1000 lb-inches, the load dependent transimission error of two such gears in mesh is of the order of 0.05°. If finite element contact analysis is to be used, the error in the transmission error due to profile discretization should be kept as low as 0.001°. Fig. 17 shows a part of the tooth profile that has been discretized. Let r_c be the radius of curvature, l be the length of the side of a typical element and ϵ be the discretization error. Then,

$$\epsilon = \frac{r_c\,(\theta/2)^2}{2} = l^2/(8r_c)$$

approximately. If we consider the part of the profile near, say, the pitch point, then the radius of curvature is

$$r_c = r_p \sin\phi = \frac{z}{2D_p}\sin\phi$$

where r_p is the pitch circle radius, ϕ is the pressure angle, z is the number of teeth and D_p is the diametral pitch. The length l of the side of a typical element is approximately

$$l = \frac{(A+B)}{D_p n},$$

where A and B are the addendum and dedendum constants of the gear, and n is the number of elements that the profile of the gear tooth spans. Therefore, the discretization error ϵ is

$$\epsilon = \frac{(A+B)^2}{4n^2 z D_p \sin\phi},$$

and the error δ in the transmission error is

$$\delta = \epsilon/r_p = \frac{(A+B)^2}{2n^2 z^2 \sin\phi} \text{ radians}$$

For δ to be of the order of 0.001° or 1.75×10^{-5} radians, the number of elements along the profile has to be n=30, and the coordinates of the nodes along the profile have to be at least as accurate as $\epsilon = 1.75 \times 10^{-5}$".

Figs. 18 and 19 show the finite element model of two gears in contact whose profiles were generated automatically by the procedure described in this article. Each gear has 32 nodes along each tooth profile.

The input gear was rotated at a constant angular speed, and a predetermined torque was applied on the output gear. Contact forces including the frictional and compressive components were computed for each position using a procedure [5] based on the Simplex algorithm, and transmission error and load-sharing information was obtained. Fig. 20 shows the computed transmission error for three different combinations of load torque M_o and frictional coefficient μ. An exaggerated value of 0.3 is chosen for the coefficient of friction to illustrate its effect on the transmission error. The transmission error curve for the light load shows ripples which may be attributed entirely to the discretization error in the profiles. In the curves for higher load, the same ripples reappear at the same places, but are much smaller than

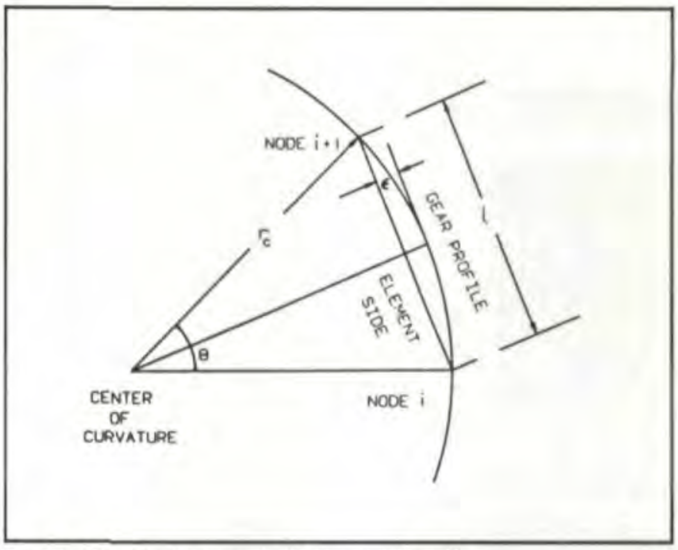

Fig. 17 – Discretization error in the gear tooth profile.

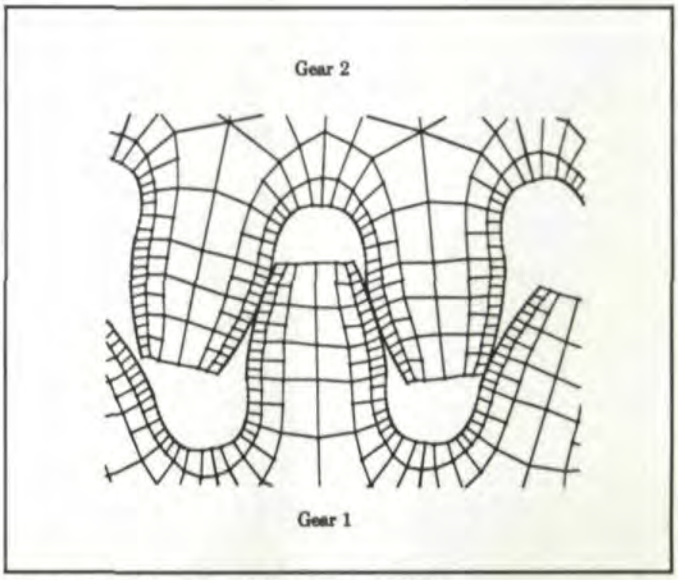

Fig. 18 – Finite element model for contact analysis.

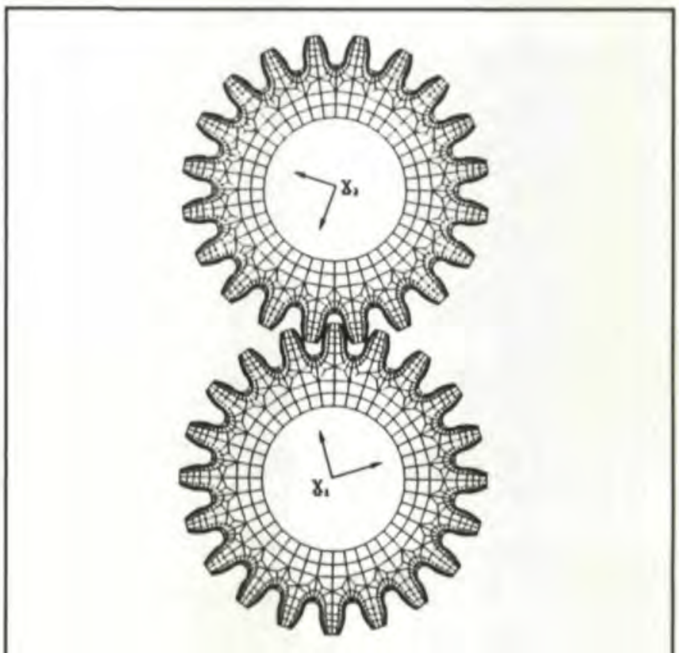

Fig. 19 – Finite element model for contact analysis.

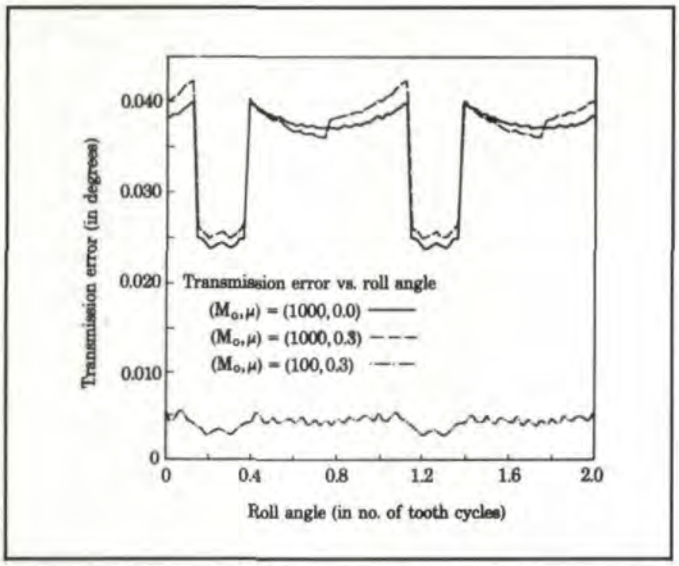

Fig. 20 – Transmission error curves obtained from finite element analysis.

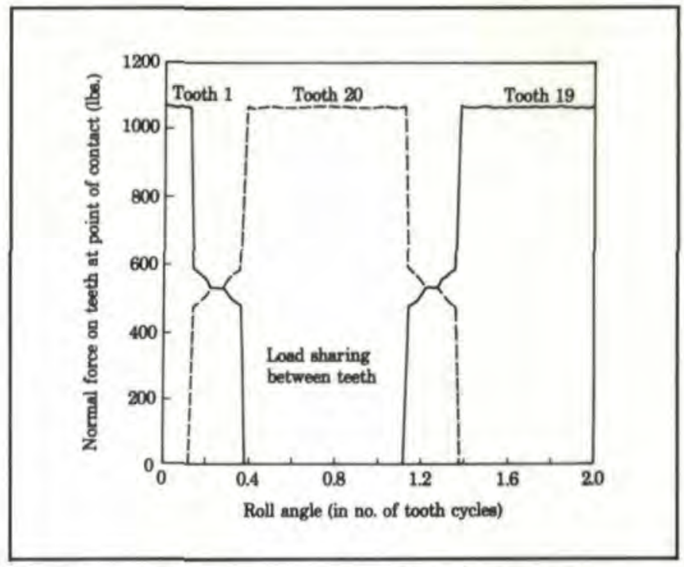

Fig. 21 – Load sharing curves obtained from finite element analysis.

the overall transmission error. Fig. 21 shows the load sharing between teeth as the gears roll through.

Conclusion

A simple, yet very general, procedure that can handle undercut as well as nonundercut gears has been described in this article. An important advantage of the method as implemented is that it is very easy to include any kind of modifications on the rack without changing the general structure of the procedure. The method has been tried out on practical applications, and the authors feel that it can be used to advantage whenever an accurate numerical description of generated gear tooth profiles is needed. A FORTRAN program has been successfully run on both an IBM PC and a VAX-11.

References

1. COLBOURNE, J.R., *The Geometry of Involute Gears*, Springer Verlag, 1987.
2. CHANG, S.H., HUSTON R.L., and COY, J.J. "A Computer Aided Design Procedure for Generating Gear Teeth", ASME Paper No. 84-DET-184.
3. HEFENG, BAI, SAVAGE, MICHAEL and KNORR, RAYMOND JAMES, "Computer Modeling of Rack-Generated Spur Gears", *Mechanisms and Machine Theory*, 20 (1985), pp. 351-360.
4. VIJAYAKAR, SANDEEP M. and HOUSER, DONALD R. "The Use of Boundary Elements for the Determination of the Geometry Factor", *Gear Technology*, Vol. 5, No. 1, Jan-Feb, 1988, pp.7ff.
5. VIJAYAKAR, SANDEEP M., BUSBY, HENRY R. and HOUSER, DONALD R. "Linearization of Multibody Contact", to appear in *Computers and Structures*, Pergamon Press, Oxford, England.

Acknowledgement:

Reprinted with permission of American Gear Manufacturers Association. The opinions, statements and conclusions presented in this article are those of the authors and in no way represent the position or opinion of the AMERICAN GEAR MANUFACTURERS ASSOCIATION.

The authors would like to thank the sponsors of the Gear Dynamics and Gear Noise Research Laboratory for their encouragement and financial support which made this study possible.